*URSI GASS 2021, Rome, Italy, 28 August - 4 September 2021*

# Localization of bars in reinforced concrete by microwaves: a quasi-quadratic inverse scattering approach

Adriana Brancaccio
Università della Campania Luigi Vanvitelli, Dipartimento di Ingegneria, Italy 81131, www.unicampania.it

## Abstract

The problem of non-destructive localization of bars in reinforced concrete is formulated for a canonical two-dimensional geometry in a ground penetrating radar measurements configuration. The knowledge of the concrete size and permittivity is exploited to obtain a quite simple approximated expression of the scattered field, where the interaction between bars and concrete is retained whereas the mutual coupling between bars is neglected. Numerical examples show the feasibility of the approach.

## 1 Introduction

Non-destructive testing (NDT) of reinforced concrete structures is of great interest in civil engineering. The bars number, diameter, and deployment, together with the concrete cover thickness, are important parameters to attest the correct structural behavior towards external mechanical stress and structure long lasting. However, it happens that the details of the structural design in terms of such parameters have been lost and must be recovered. Moreover, structure can be damaged during its life for concrete corrosion or if some of the bars are oxidized, so showing a diameter less than the nominal one, or lack at all. So, the need of NDT for diagnostic and continuous monitoring purposes arises.

Microwave tomography has been proposed in the past and in recent years as a suitable technique to these scopes [1-4]. Many papers assume, implicitly or explicitly, a linear approximation of the scattering. This choice allows to deal with inverse problems where the attainable resolution can be forecast and well assessed techniques against noise are at hand. However, linear approximations neglect mutual interactions inside the structure.
On the other hand, a moderate degree of non-linearity, i.e., a quadratic approximation of the scattering phenomenon, has demonstrated to be a good compromise between the full nonlinear problem, that usually does not present global convergence to the solution, and the rough linear one [5,6]. Also, when dealing with structures that are partially known, a formulation that includes all the a priori information can be helpful. This approach was considered in [7,8] where a linear approximation has been adopted.

A further element that must be considered is the measurement configuration. A full view illumination allows to collect more information with respect to a limited aspect one. However, sometimes the structure is not accessible from all around and only a reflection mode illumination, typical for instance of ground penetrating radar applications, is allowed. Here, this last case is considered.

In this brief contribution the problem is formulated in a canonical geometry. It is assumed to deal with rectangular concrete pillars, whose section is the domain that must be investigated. A scalar two-dimensional formulation is adopted, where the electric field polarization is parallel to the vertical bars. An "almost" quadratic approximation of the direct problem is derived, that allows to achieve, for the geometry at hand, a synthetic formulation where the involved coefficients can be evaluated analytically, thus reducing computing burden.

The concrete is represented as a lossless homogeneous medium and the bars as electrical conducting cylinders with circular cross section whose radius is known. Realistic values of the pillar dimension and of the bars diameter, number and position, have been assumed for the numerical example reported in the following. The structure is tested by means of incident fields, radiated by filamentary electric sources placed at different positions along a straight segment outside the investigated region. The datum of the problem is the multi-monostatic scattered field observed at different frequencies. The problem is formulated as the detection and localization of an unknown number of scatterers inside a pre-determined grid of "candidate" positions. The result of the inversion algorithm is an image showing spots where bars have been detected.

## 2 Formulation

The geometry of the problem is depicted in Figure 1. The investigation domain (ID) is represented by the rectangle $ID = [-X_c, X_c] \times [z_{min}, z_{max}]$, whose relative permittiviy $\varepsilon_c$ is constant (except for the bars). Inside ID there are $N$ circular cylindrical bars of radius $r_b$, conductivity $\sigma$ and positions $\boldsymbol{r}_n = (x_n, z_n)$, $n = 1, \dots, N$. A $y$-polarized line source moves along the measurement line within the interval $[-X_s, X_s]$ and a multi-monostatic configuration is assumed where measurements of the scattered electric field $E_s$ are collected at the same source positions at different frequencies, corresponding to the free space wavenumber $k_0$. As it is well known the scattering equations are:

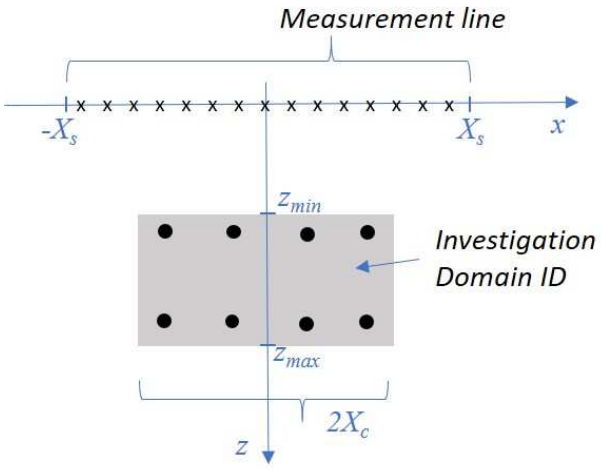


**Figure 1.** Geometry of the problem and absolute reference system. Source and receiver move along the measurement line.

$$E_s = \mathcal{A}_e[\chi E]$$
$$E = E_i + \mathcal{A}_i[\chi E] \tag{1}$$

where $E_i$ and $E$ are the incident and the total field *inside* the (not accessible) investigation domain respectively, $\chi$ is the normalized contrast between the investigation domain equivalent permittivity and the external region one, and $\mathcal{A}_e$, $\mathcal{A}_i$ are linear operators whose kernel is the Green's function of the scattering problem, calculated outside and inside ID respectively. In the two-dimensional case, it results:

$$\mathcal{A}_e[f] = -j\frac{k_0^2}{4}\iint_{ID} H_0^{(2)}(k_0 R_e)\, f(x',z')dx'dz', \tag{2}$$

$$\mathcal{A}_i[f] = -j\frac{k_0^2}{4}\iint_{ID} H_0^{(2)}(k_0 R_i)\, f(x',z')dx'dz', \tag{3}$$

$$E_i = -\frac{k_0\,\zeta_0}{4} H_0^{(2)}(k_0 R_e), \tag{4}$$

where $R_e = \sqrt{(x-x')^2 + (z')^2}$ with $x \in [-X_s, X_s]$, $R_i = \sqrt{(x-x')^2 + (z-z')^2}$ with $(x,z) \in ID$, $\zeta_0$ is the free space impedance, $H_0^{(2)}$ is the zero order Hankel function of second kind, and unitary current source is assumed.
The relationship between contrast and scattered field can be approximated as [6]:

$$E_s = \mathcal{A}_e[\chi E_i] + \mathcal{A}_e\big[\chi\mathcal{A}_i[\chi E_i]\big]. \tag{5}$$

In the proposed approach, the contrast is expressed as:

$$\chi(x,z) = \chi_c - jF_b(x,z), \quad (x,z) \in ID, \tag{6}$$

where $\chi_c = \varepsilon_c - 1$ is constant over ID and

$$F_b(x,z) = \frac{\sigma\zeta_0}{k_0}\sum_{n=1}^{N}\varphi(|\boldsymbol{r} - \boldsymbol{r}_n|), \tag{7}$$

with

$$\varphi(r) = \begin{cases} 0 & r > r_b \\ 1 & r \le r_b \end{cases} \tag{8}$$

In this way, the contributions of the concrete and of the bars to the linear term of the scattering operator (5) can be separated. The quadratic term is here approximated further by neglecting the mutual product $F_b(x,z)F_b(x',z')$ in the related integrals. This entails to neglect mutual interaction between the bars, while retaining the interaction between bars and concrete:

$$\hat{E}_s \triangleq E_s - \{\chi_c\mathcal{A}_e[E_i] + \chi_c^2\mathcal{A}_e\big[\mathcal{A}_i[E_i]\big]\} = -j\mathcal{A}_e[F_b E_i] - 2j\chi_c\mathcal{A}_e\big[\mathcal{A}_i[F_b E_i]\big]. \tag{9}$$

Finally, considering Eqs. (2)-(4) and (7), it can be shown, after some non-trivial passages, skipped here for sake of brevity, that Eq. (9) can be made explicit as:

$$\hat{E}_s(k_0,x) = \sum_{n=1}^{N} C_n(k_0)\big[H_0^{(2)}\big(k_0\sqrt{(x-x_n)^2 + (z_n)^2}\big)\big]^2. \tag{10}$$

Eq. (10) appears relatively simple. The coefficients $C_n$ do not depend on the source position. Their expression is:

$$C_n(k_0) = \pi r_b^2\frac{k_0^2\zeta_0^2\sigma}{16}\Big\{1 - 2j\chi_c + 2j\chi_c J_0(k_0 r_b) + \chi_c\frac{k_0}{r_b}J_1(k_0 r_b)A_n\Big\}, \tag{11}$$

where $J_v$ represents the Bessel function of $v$ order and

$$A_n = \int_0^{2\pi}\frac{r(\vartheta)^2}{2}[J_0(k_0 r(\vartheta))H_0(k_0 r(\vartheta)) + J_1(k_0 r(\vartheta))H_1(k_0 r(\vartheta))]d\vartheta, \tag{12}$$

where $r(\vartheta)$ is the maximum distance of center of the *n-th* bar from the ID border, in the direction $\vartheta$ (look Figure 2). Note that $A_n$ accounts for the bars position inside ID. Integral in Eq. (12) must be calculated numerically.

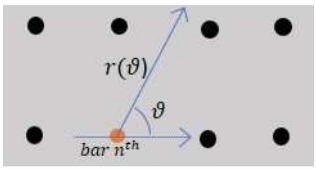


**Figure 2.** Reference system relative to n-th bar, used to compute the integral in Eq. (12).

Equation (10) allows to formulate the inverse problem as the detection and localization of bars between a pre-defined number $N_B > N$ of "candidate" positions. Let us define the discrete function $\gamma(n)$ whose value is 1 if the *n-th* position corresponds to the presence of a bar, otherwise it is equal to 0. In this way, the problem can be recast as the inversion of the following linear equation:

$$\hat{E}_s((k_0, x_s) = \sum_{n=1}^{N_B} C_n\left[H_0^{(2)}\left(k_0\sqrt{(x_s - x_n)^2 + (z_n)^2}\right)\right]^2 \gamma(n). \quad (13)$$

where $\gamma(n)$ plays the role of the unknown.

## 3 Numerical results

The following example refers to the configuration reported in Table 1. The scattered field is numerically simulated at $N_f$ equispaced frequencies and $N_X$ equally spaced positions along the measurement line.

**Table 1.** Direct problem simulation parameters

| parameter | Symbol | value |
|---|---|---|
| Concrete contrast | $\chi_c$ | 3 |
| Number of bars | $N$ | 8 |
| bars positions | $(x_n, z_n)$ | Look Figure 3 (red circles) |
| Bars' radius | $r_b$ | 8mm |
| ID width | $2X_c$ | 40cm |
| ID depth | $z_{min} - z_{max}$ | 25cm |
| ID distance from the measurement line | $z_{min}$ | 25cm |
| Frequency band | $[f_{min}, f_{max}]$ | $[0.62, 2.90]GHz$ |
| Number of frequencies | $N_f$ | 45 |
| Measurement line extent | $2X_s$ | 100cm |
| Number of measurement points | $N_X$ | 51 |

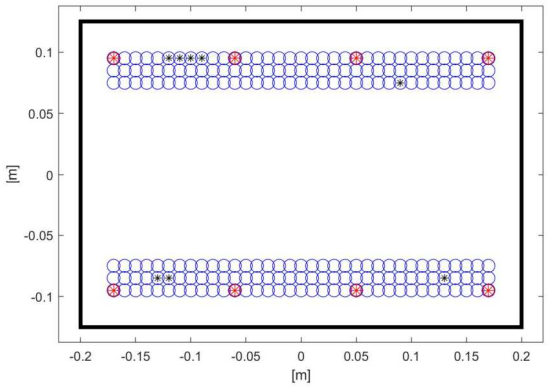


**Figure 3.** Example of bars detection, the investigation domain is denoted by the black edge rectangle: "candidate" positions (blue circles); actual positions (red circles); detected position by the quasi-quadratic model inversion (red stars); detected positions by the linear model (black stars).

The inversion has been performed by assuming $N_B = 210$ candidate positions, indicated by the blue circles in Figure 3. In the same Figure the actual bars position is indicated by red circle and the recovered ones, estimated by inverting the model in Eq. (13), are depicted with red stars. As it can be appreciated, the actual bars position and presence are well recovered. For comparison purposes, the same scattered field data have been inverted by using a simpler "linear" model, obtained by retaining only the first term in the last member of Eq. (9). The corresponding result, that does not provide the desired detection and localization, is depicted by the black stars, reported again in Figure 3.

## 7 References


1. C. Pichot, P. Trouillet, "Diagnosis of Reinforced Structures: An Active Microwave Imaging System," In: Nowak A.S. (eds) Bridge Evaluation, Repair and Rehabilitation. NATO ASI Series (Series E: Applied Sciences), **187**, Springer, Dordrecht, 1990, pp.201-215, doi:10.1007/978-94-009-2153-5_15

2. G. Leucci, "Electromagnetic monitoring of concrete structures," *Proceedings of the XIII Internarional Conference on Ground Penetrating Radar*, Lecce, 2010, pp. 1-5, doi: 10.1109/ICGPR.2010.5550230.

3. J. Stryk, A.M. Alani, R. Matula, K. Pospisil, "Innovative Inspection Procedures for Effective GPR Surveying of Critical Transport Infrastructures (Pavements, Bridges and Tunnels)," In: Benedetto A., Pajewski L. (eds) Civil Engineering Applications of Ground Penetrating Radar. Springer Trans. in Civil and Environ. Eng., Springer, Cham, 2015, pp. 71-95, doi:10.1007/978-3-319-04813-0_3.

4. V. Chandrasekaran, "Tomography of reinforced concrete," *Mat Design Process Comm.*, 2019, doi:10.1002/mdp2.92.

5. R. Pierri, A. Brancaccio, "Imaging of a rotationally symmetric dielectric cylinder by a quadratic approach," *J. of Opt. Soc. of America A*, **14**, 10, Oct. 1997, pp. 2777-2785, doi:10.1364/JOSAA.14.002777.

6. G. Leone, A. Brancaccio, R. Pierri, "Linear and quadratic inverse scattering for angularly varying circular cylinders," *J. of Opt. Soc. of America A*, **16**, 12, Dec. 1999, pp. 2887-2895, doi:10.1364/JOSAA.16.002887.

7. A. Brancaccio, G. Leone, R. Solimene; "Fault detection in metallic grid scattering," *J. of Opt. Soc. of America A*, **28**, 12, Dec. 2011, pp. 2588-2599, doi: 10.1364/JOSAA.28.002588.

8. A. Brancaccio and R. Solimene, "Fault detection in dielectric grid scatterers", *Optic Express*, **23**, 2015, p. 8200-8215, doi: 10.1364/OE.23.008200.